Charge Self-compensation in the Nonlinear Optical Crystals $Rb_{0.855}Ti_{0.955}Nb_{0.045}OPO_4$ and $RbTi_{0.927}Nb_{0.056}Er_{0.017}OPO_4$

J. J. Carvajal,[†] J. L. García-Muñoz,[‡] R. Solé,[†] Jna. Gavaldà,[†] J. Massons,[†]
X. Solans,[§] F. Díaz,[†] and M. Aguiló*,[†]

*Física i Cristal·lografia de Materials i IEA, Universitat Rovira i Virgili,
43005 Tarragona, Spain, Institut de Ciència de Materials de Barcelona,
C.S.I.C., Campus Universitari de Bellaterra, 08193 Bellaterra, Spain, and Departament de
Cristal·lografia i Mineralogia, Universitat de Barcelona, 08028 Barcelona, Spain*

We used X-ray single-crystal diffraction (XRD) and high-resolution neutron powder diffraction (NPD) and performed second-harmonic generation (SHG) measurements to investigate the structural details and nonlinear optical (NLO) properties of $Rb_{0.855}Ti_{0.955}Nb_{0.045}OPO_4$ and $RbTi_{0.927}Nb_{0.056}Er_{0.017}OPO_4$. We studied in detail the distribution of Nb^{5+} and Er^{3+} doping cations among the different types of TiO_6 octahedra in the structure. We found that Nb cations exclusively occupied Ti(1) sites, but we did not observe a preferential occupation of the octahedra by Er. Our results established that, in $Rb_{0.855}Ti_{0.955}Nb_{0.045}OPO_4$, the substitution of Ti^{4+} by Nb^{5+} centers was compensated by the creation of Rb^+ vacancies. The SHG measurements in these crystals reveal that these crystals are excellent nonlinear optical materials and that the absorption of the generated green light by Er^{3+} in the $RbTi_{0.927}Nb_{0.056}Er_{0.017}OPO_4$ crystal is negligible.

Introduction

Potassium titanyl phosphate, $KTiOPO_4$ (KTP), is the best-known member of the family of compounds with formula $MM'OXO_4$ (M = K, Rb, Tl, Na, NH$_4$ or Cs; M′ = Ti, Ge, Sn; and X = P or As; or partial substitution in M and M′ by two or more different cations).[1,2] Many of the crystals in this family are interesting because of their nonlinear optical (NLO) properties. KTP is particularly interesting for its application in the second-harmonic generation of 1.064-μm Nd lasers.[3] All members of this family are orthorhombic, biaxial crystals and belong to the noncentrosymmetric space group *Pna*2$_1$ (point group *mm*2). The structure is characterized by helicoidal chains of $M'O_6$ octahedra that are linked between them at two corners and separated by XO_4 tetrahedra.[4]

Many isostructural analogues have been synthesized.[5] This family of compounds is therefore particularly good for investigating the relationship between crystal structure and optical properties. Several isomorphous substitutions have been made in the KTP structure to determine the origin of its NLO properties. A few substitutions have maintained or improved the second-harmonic generation (SHG) response of KTP.[6] The main reason for this seems to be the deformation of the $M'O_6$ octahedra: the more distorted these octahedral are, the higher the efficiency of SHG of the material.[7,8]

Niobium is known to substitute isomorphously for Ti in a number of mixed-titanate compounds such as KTP:Nb[6] or K(TiNb)O5.[9] This last family of compounds, with a different structure from that of KTP, can be made nonstoichiometric with a chemical formula of the type $K_{1-x}(Ti_{1-x}Nb_{1+x})O_5$.[10] In both structures, the presence of Nb is compensated by vacancies in the K site. In the case of Nb^{5+}, many different types of charge compensators were reported with the KTP structure: first, on the octahedral site by Ga^{3+} with a partial charge compensation and K^+ vacancies induced[11] and Mg^{2+} in $K(Ti_{1-x}(Mg_{1/3}Nb_{2/3})_x)OPO_4$ without induction of K^+ vacancies;[12] second, on the tetrahedral site, by Si^{4+} with the structure $K_{1.16}(Ti_{0.37}Nb_{0.63})(Si_{0.63}P_{0.53})O_{5.48}$.[13] Also, Ti^{4+} cations in $KTiOAsO_4$ (KTA) crystals can be completely substituted with $(Nb^{5+}-M^{3+})$[14] cation pairs

* Corresponding author: aguilo@quimica.urv.es.
† Universitat Rovira i Virgili.
‡ Campus Universitari de Bellaterra.
§ Universitat de Barcelona.
(1)] Masse, R.; Grenier, J. C. *Bull. Soc. Fr. Minéral. Cristallogr.* **1971**, *94*, 437.
(2) Hagerman, M. E.; Poeppelmeier, K. R. *Chem. Mater.* **1995**, *7*, 602.
(3) Satyanarayan, M. N.; Deepthy, A.; Bhat, H. L. *Crit. Rev. Solid State Mater. Sci.* **1999**, *24*, 103.
(4) Thomas, P. A.; Mayo, S. C.; Watts, B. E. *Acta Crystallogr.* **1992**, *B48*, 401.
(5) Stucky, G. D.; Phillips, M. L. F.; Gier, T. E. *Chem. Mater.* **1989**, *1*, 492.

(6)] Thomas, P. A.; Watts, B. E. *Solid State Commun.* **1990**, *73*, 97.
(7)] Voronkova, V. I.; Yanovskii, V. K.; Sorokina, N. I.; Verin, I. A.; Simonov, V. I. *Crystallogr. Rep.* **1993**, *38*, 662.
(8)] Voronkova, V. I.; Yanovskii, V. K.; Verin, I. A.; Vigdorchik, A. G.; Simonov, V. I. *Crystallogr. Rep.* **2000**, *45*, 386.
(9) Wadsley, A. D. *Acta Crystallogr.* **1964**, *17*, 623.
(10) Rebbah, H.; Desgardin, G.; Raveau, B. *J. Solid State Chem.* **1980**, *31*, 321.
(11)] Blasse, G.; Brihner, L. H. *Matter. Res. Bull.* **1989**, *24*, 1099.
(12)] McCarron, E. M., III; Calabrese, J. C.; Gier, T. E.; Cheng, L. K.; Foris, C. M.; Bierlein, J. D. *J. Solid State Chem.* **1993**, *102*, 354.
(13)] Chani, V. I.; Shimamura, K.; Endo, S.; Fukuda, T. *J. Cryst. Growth* **1997**, *171*, 472.

(with M = Al, Cr, Ga, Fe, In) on the octahedral site and it seems to be that Ti^{4+} can be completely substituted by Nb^{5+} when Ge^{4+} substituted As in the tetrahedral site in KTA crystals.[14] It was demonstrated that the KTA matrix was more stable for this substitution than the KTP matrix because the corresponding $K(Nb^{5+},M^{3+})$-OPO_4 phase was not observed. Cheng et al.[15] reported that substituting the Ti^{4+}–K^+ pair with Nb^{5+} in the KTP crystal increases the optical birefringence and makes the material suitable for the SHG of blue light. Wei et al.[16] reported noncritical phase matching from YAG:Nd 1.06-μm laser in 4.0% KTP:Nb crystal and obtained 4% efficiency in their first experiment. Our study deals with the preparation of solid solution crystals of the $RbTiOPO_4$ family, obtained from the substitution of Ti^{4+} with (Nb^{5+}–Ln^{3+}).

Doping these crystals with lanthanide (Ln^{3+}) ions is interesting because the ion photoluminescence and the NLO properties of the matrix can be merged to achieve self-induced effects. In previous studies,[17–19] we showed that when we used RTP crystals doped with Nb as a matrix to host Ln^{3+}, an Er^{3+} concentration similar to that obtained in other laser matrixes was achieved. Er^{3+} is interesting because of its emission around 1.5 μm.[20] This ion is used in optical communications at long distances because of its efficient emission near the region of losses in silica fibers.[21] It is also used in medicine because of its emission at around 2.8 μm.[22]

In this study, we have refined the structure of two new crystals: $Rb_{0.855}Ti_{0.955}Nb_{0.045}OPO_4$ and $RbTi_{0.927}$-$Nb_{0.056}Er_{0.017}OPO_4$. We paid particular attention to the positions occupied by dopant cations Nb and Er in the structure and measured the SHG efficiency in both materials. Finally, we compared our results with those of other members of this family and their respective NLO properties.

Experimental Procedures

Crystal Growth. $RbTiOPO_4$ doped with Nb (RTP:Nb) and co-doped with Nb and Er (RTP:(Nb,Er)) were obtained from solutions of molar composition Rb_2O–P_2O_5–TiO_2–Nb_2O_5–Er_2O_3 = 42.9–35.1–19.8–2.2–0 and 42.0–28.0–27.6–1.5–0.9, respectively, by spontaneous nucleation on a Pt wire. The experiments were carried out in a vertical tubular furnace controlled by a Eurotherm 818P controller/programmer using 25-cm^3 platinum crucibles filled with about 15 g of solution. Rb_2CO_3, $NH_4H_2PO_4$, TiO_2, Nb_2O_5, and Er_2O_3 (p.a.) were used as initial reagents, mixed in the desired ratios, and heated until bubbling of NH_3, H_2O, and CO_2 was complete. The solution was homogenized by maintaining the temperature at

about 50–100 K above the expected saturation temperature for 3–5 h, 1190 and 1180 K being the saturation temperatures of RTP:Nb and RTP:(Nb,Er) crystals, respectively. The difference in temperature between the surface of the solution and the bottom of the crucible was about 15 K. The temperature of the homogeneous solution was lowered in 10 K steps every 30 min, until crystals appeared on the platinum wire immersed in the solution. Then, we replaced the platinum wire with a platinum disk in contact with the surface of the solution to obtain larger crystals. After that, the temperature was decreased 20 K at a rate of 2.5 K/h to obtain the crystals with good enough quality and quantity for the latter characterizations. The quality of the crystallized phases was first checked by laboratory X-ray powder diffraction using a Siemens D5000 powder diffractometer.

Dopant Concentration Analyses. The crystals obtained were cleaned and analyzed by electron probe microanalysis (EPMA) to determine the concentration of the doping elements. A CAMECA SX-50 operating in wavelength dispersive mode was used. The samples were included in a polyester ortoftalic-type resin and the surfaces of the samples were polished using diamond powders until a grain size of 1 μm was reached. The concentrations of Rb, Ti, P, Nb, and O were analyzed at an electron current of 30 nA and the concentration of Er was analyzed at 100 nA. In all cases, the accelerating voltage was maintained at 25 kV. The raw intensities were corrected for dead time, background, and matrix effects using the PAP correction procedure.[23] The error in the determination of the content of Rb, Ti, and P in the samples in weight percent were around 1%, for Nb and O were around 3%, and for Er was around 15%. The cation concentrations from these analyses were taken as the nominal compositions in the two types of crystals of this work.

Single-Crystal X-ray Diffraction. A small piece of an as-grown crystal of RTP:Nb was selected (to avoid defects that are easily introduced in the material by cutting and polishing) to determine its single-crystal X-ray structure (XRD). Single-crystal XRD measurements were carried out at RT, and the structure was resolved by Patterson synthesis. Details of crystal data, data collection, and refinement are given in Table 1.

Neutron Powder Diffraction. Neutron powder diffraction (NPD) measurements on RTP:(Nb,Er) were taken with the D2B high-resolution diffractometer at the Institut Laue Langevin (Grenoble, France). This diffractometer is equipped with a bank of 64 detectors separated by 2.5° 2θ, spanning an angular range of 160°. A good quality pattern was obtained at room temperature (RT) in the high-flux mode of D2B (see Figure 1). The wavelength used was 1.594 Å and the counting time was run about 3 h to have the desired statistics over the angular range 0–160° 2θ. NPD data were analyzed by the Rietveld method, using the refinement program FULLPROF.[24]

Second-Harmonic Generation. The SHG properties of these crystals were studied by a powder technique.[25] The samples, powdered and graded between 5 and 20 μm by standard sieves, were loaded into a 2-mm-thick quartz cell using a vibrator to ensure uniform packing. The powder was illuminated with a YAG:Nd pulsed laser. We estimated the fundamental power by measuring the 1064-nm energy reflected by the sample. The back-scattered harmonic power generated by the sample was collected using a lens and focused on a Si detector. We analyzed intersignals using a digital oscilloscope and used the ratio between the two maxima to describe the SHG efficiency process. This ratio was averaged over 100 laser shots. With this method we cannot measure the absolute efficiency of the SHG of the samples, so we compared this ratio with that of pure KTP, whose SHG efficiency is well-established in the literature.[26]

(14)] Chani, V. I.; Shimamura, K.; Endo, S.; Fukuda, T. *J. Cryst. Growth* **1997**, *173*, 117.

(15) Cheng, L. T.; Cheng, L. K.; Harlow, R. L.; Bierlein, J. D. *Appl. Phys. Lett.* **1994**, *64*, 155.

(16) Wei, J. Q.; Wang, J. Y.; Liu, Y. G.; Wang, C. Q.; Shao, Z. S.; Guan, Q. C.; Jiang, M. H. *Chin. Phys. Lett.* **1996**, *13*, 203.

(17) Carvajal, J. J.; Nikolov, V.; Solé, R.; Gavaldà, Jna.; Massons, J.; Rico, M.; Zaldo, C.; Aguiló, M.; Díaz, F. *Chem. Mater.* **2000**, *12*, 3171.

(18) Carvajal, J. J.; Solé, R.; Gavaldà, Jna.; Massons, J.; Rico, M.; Zaldo, C.; Aguiló, M.; Díaz, F. *J. Alloys Compd.* **2001**, *323–324*, 231.

(19) Carvajal, J. J.; Solé, R.; Gavaldà, Jna; Massons, J.; Aguiló, M.; Díaz, F. *Cryst. Growth Des.* **2001**, *1*, 479.

(20) Kaminskii, A. A. *Crystalline Lasers: Physical Processes and Operating Schemes*; CRC Press: Boca Raton, FL, 1996.

(21) Dominiak-Dzik, G.; Golab, S.; Pracka, I.; Ryba-Romanowski, W. *Appl. Phys. A* **1994**, *58*, 551.

(22) Koechner, W. *Solid-State Laser Engineering*; Springer Series in Optical Sciences; Springer-Verlag: Berlin, 1996; pp 63–66.

(23) Pouchou, J. L.; Pichoir, F. *Rech. Aerosp.* **1984**, *3*, 13.

(24) Rodríguez-Carvajal, J. *Physica B* **1993**, *192*, 55.

(25) Kurtz, S. K.; Perry, T. T. *J. Appl. Phys.* **1968**, *39*, 3798.

(26) Dmitriev, V. G.; Gurzadyan, G. G.; Nikogosyan, D. N. *Handbook of Nonlinear Optical Materials*; Springer-Verlag: New York, 1991.

Table 1. Crystal Data, Data Collection, and Refinement of $Rb_{0.855}Ti_{0.955}Nb_{0.045}OPO_4$ by X-ray Single-Crystal Diffraction

Crystal Data

$Rb_{0.855}Ti_{0.955}Nb_{0.045}OPO_4$	Mo Kα radiation
formula weight = 233.81	$\lambda = 0.71069$ Å
orthorhombic	cell parameters from 25 reflections
$Pna2_1$	$\theta = 12-21°$
$a = 12.947(3)$ Å	$\mu = 11.495$ mm^{-1}
$b = 6.498(3)$ Å	
$c = 10.579(7)$ Å	
$\alpha = \beta = \gamma = 90°$	$T = 293(2)$ K
	equidimensional
	0.2-mm diameter
$V = 890.0(7)$ Å^3	colorless
$Z = 8$	
$D_x = 3.490$ Mg m^{-3}	
$D_m =$ (not measured)	

Data Collection

Enraf-Nonius CAD-4	$R_{int} = 0.035$
$\omega/2\theta$ scan	$\theta_{max} = 29.95°$
absorption correction: φ-scan	$h = 0-18$
1382 measured reflections	$k = 0-9$
1360 independent reflections	$l = 0-14$
1114 reflections with $I > 2\sigma(I)$	

Refinement

refinement on F^2 $R[F^2 > 2\sigma(F^2)] = 0.0328$	$\Delta\rho_{max} = 0.646$ e Å^{-3}
$wR(F^2) = 0.0788$	$\Delta\rho_{min} = -0.354$ e Å^{-3}
$S = 1.019$	
1360 reflections	
148 parameters	Flack absolute structure parameter = $-0.027(14)$
$w = 1/[\sigma^2(F_o^2) + (0.0469P)^2]$	scattering factors from *International Tables*
where $P = (F_o^2 + 2F_c^2)/3$	*for Crystallography* (vol. C)

Results

Structural Characterization. The crystals obtained had the characteristic shape of RTP crystals. There was only one difference: doping with niobium flattened them somewhat, as we explained in detail in a previous study.[17] The as-grown crystals were light gray-bluish, but this color disappeared after an additional 3 h of annealing of the crystal in air at 773 K. In crystals containing Er, the characteristic pale pink color of this ion remained, while RTP:Nb crystals were colorless or pale yellow. The samples were free of impurities and the structural refinements of single-crystal XRD and NPD data were performed in the orthorhombic $Pna2_1$ space group.

$Rb_{0.855}Ti_{0.955}Nb_{0.045}OPO_4$ Structure. We solved the structure of $Rb_{0.855}Ti_{0.955}Nb_{0.045}OPO_4$. The unit cell parameters were $a = 12.947(3)$ Å, $b = 6.498(3)$ Å, and $c = 10.579(7)$ Å and $Z = 8$. Parameter a was shorter, b was slightly longer, and c was clearly longer than the corresponding ones in the RTP structure. Details of crystal data, refinement, and atomic coordinates are given in Tables 1 and 2.

The main characteristic of this structure is that we obtained the enantiomorphic image of pure RTP. This means that while the x and y coordinates for all the atoms did not change very much, the z coordinates shifted considerably and were related to the z coordinate of pure RTP structure with a mirror plan at a height of practically a quarter in the c direction. This feature was also observed in the KTP:Nb structure when it was compared to that of pure KTP.[6,27]

Table 3 shows the occupation factors of the $Rb_{0.855}$-$Ti_{0.955}Nb_{0.045}OPO_4$ structure. The occupancies of the crystallographically independent positions for rubidium

cations were 0.832(5) for Rb(1) and 0.878(5) for Rb(2). This follows the same trend as in the KTP:Nb samples.[27] The occupancies of Ti sites were 0.910(8) and 0.090(8) for Ti and Nb, respectively, in Ti(1) positions and 1.000-(8) and 0.000(8) for the same cations in Ti(2) positions. We refined the Ti occupancies by assuming that each of these positions were fully occupied by titanium and niobium atoms. There is a tendency for Nb to occupy only the Ti(1) position.

The anisotropic displacements parameters of the atoms are given in Table 4.

$RbTi_{0.927}Nb_{0.056}Er_{0.017}OPO_4$ Structure. We used the structure of $Rb_{0.855}Ti_{0.955}Nb_{0.045}OPO_4$ as a starting model to refine the structure of the $RbTi_{0.927}Nb_{0.056}Er_{0.017}OPO_4$ crystal by NPD. By carefully analyzing high-resolution NPD data, we were able to study fine structural details such as oxygen positions and, in particular, to determine the location of dopants. In the refinements we used a pseudo-Voigt profile function corrected for asymmetry and a six-parameter polynomial function to reproduce the background.

Table 5 shows the RT cell parameters, refined atomic coordinates, and isotropic temperature factors of $RbTi_{0.927}$-$Nb_{0.056}Er_{0.017}OPO_4$ structure from NPD. It also shows the final reliability factors. Figure 1 illustrates the agreement between the observed and calculated NPD profiles. The high-angle region of the refined NPD pattern (see Figure 1b) illustrates the excellent agreement between the observed and calculated NPD profiles for the best fit, which provide the occupations shown in Table 3.
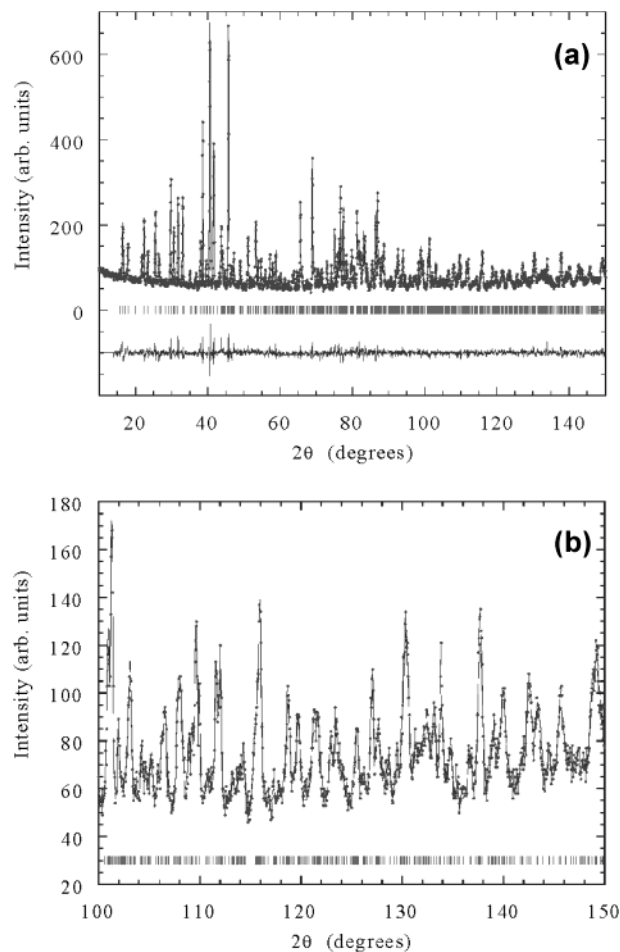
(27) Losevskaya, T. Y.; Alekseeva, O. A.; Yanovskii, V. K.; Voronkova, V. I.; Sorokina, N. I.; Simonov, V. I.; Stefanovich, S. Y.; Ivanov, S. A.; Eriksson, S.; Zverkov, S. A. *Crystallogr. Rep.* **2000**, *45*, 739.

D *Chem. Mater.*   *Carvajal et al.*

Figure 1. (a) Refined neutron diffraction pattern of $RbTi_{0.927}Nb_{0.056}Er_{0.017}OPO_4$ showing the observed (points), calculated (full line), and difference (bottom) Rietveld profiles at RT (D2B data). (b) Detail of the high-angle region of the refined neutron diffraction pattern.

Table 2. Atomic Coordinates and Equivalent Isotropic Displacement Parameters of $Rb_{0.855}Ti_{0.955}Nb_{0.045}OPO_4$ from X-ray Single-Crystal Diffraction

Cell Parameters			
a (Å) = 12.947(3)	b (Å) = 6.498(3)	c (Å) = 10.579(7)	V (Å^3) = 890.0(7)

atom	x	y	z	U(eq)
Ti(1)	0.3726(1)	0.5001(1)	0.4438(1)	0.021(1)
Nb(1)	0.3726(1)	0.5001(1)	0.4438(2)	0.021(1)
Ti(2)	0.2485(1)	0.2660(2)	0.6950(1)	0.018(1)
P(1)	0.4997(2)	0.3350(2)	0.7001(2)	0.038(1)
P(2)	0.1810(1)	0.5015(3)	0.9530(2)	0.050(1)
Rb(1)	0.3862(1)	0.7852(2)	0.7666(1)	0.042(1)
Rb(2)	0.1045(1)	0.6896(2)	0.5173(1)	0.039(1)
O(1)	0.4882(4)	0.4773(10)	0.5878(6)	0.041(1)
O(2)	0.5129(5)	0.4638(11)	0.8243(5)	0.042(1)
O(3)	0.4008(5)	0.2070(9)	0.7182(6)	0.043(1)
O(4)	0.5945(4)	0.1909(8)	0.6756(5)	0.040(1)
O(5)	0.1124(4)	0.3128(8)	0.9829(5)	0.040(1)
O(6)	0.1128(4)	0.6928(9)	0.9275(7)	0.037(1)
O(7)	0.2510(5)	0.5466(9)	1.0688(5)	0.041(1)
O(8)	0.2516(5)	0.4615(9)	0.8416(6)	0.045(1)
OT(1)	0.2210(5)	0.9611(9)	1.0833(5)	0.043(1)
OT(2)	0.2240(5)	0.0479(10)	0.8317(5)	0.045(1)

Table 3. Occupation Factors at the Ti and Rb Sites in $Rb_{0.855}Ti_{0.955}Nb_{0.045}OPO_4$ and $RbTi_{0.927}Nb_{0.056}Er_{0.017}OPO_4$

	occupation factor	
atom	$Rb_{0.855}Ti_{0.955}Nb_{0.045}OPO_4$ from X-ray single-crystal diffraction	$RbTi_{0.927}Nb_{0.056}Er_{0.017}OPO_4$ from neutron powder diffraction
Ti(1)	0.910(8)	0.871(6)
Nb(1)	0.090(8)	0.111(6)
Er(1)		0.017(6)
Ti(2)	1.000(8)	0.983(6)
Nb(2)	0.000(8)	0.000(6)
Er(2)		0.017(6)
Rb(1)	0.832(5)	1.000(4)
Rb(2)	0.878(5)	1.000(4)

Table 4. Anisotropic Displacement Parameters (Å^2) of Orthorhombic $Rb_{0.855}Ti_{0.955}Nb_{0.045}OPO_4$; Anisotropic Displacement Factor Exponent Takes the Form $-2\pi^2[h^2a^{*2}U_{11}+ ... + 2hka^*b^*U_{12}]$

| atom	U_{11}	U_{22}	U_{33}	U_{23}	U_{13}	U_{12}
Ti(1)	0.022(1)	0.015(1)	0.026(1)	0.001(1)	−0.001(1)	0.000(1)
Nb(1)	0.022(1)	0.015(1)	0.026(1)	0.001(1)	−0.001(1)	0.000(1)
Ti(2)	0.018(1)	0.015(1)	0.021(1)	−0.002(1)	0.000(1)	−0.001(1)
P(1)	0.037(1)	0.032(1)	0.046(1)	0.001(1)	−0.001(1)	0.001(1)
P(2)	0.062(1)	0.034(1)	0.056(1)	0.000(1)	0.001(1)	−0.001(1)
Rb(1)	0.045(1)	0.027(1)	0.054(1)	0.001(1)	0.004(1)	0.003(1)
Rb(2)	0.032(1)	0.033(1)	0.050(1)	0.002(1)	0.001(1)	0.004(1)
O(1)	0.036(2)	0.042(3)	0.048(3)	0.004(2)	0.001(2)	−0.002(2)
O(2)	0.024(3)	0.048(3)	0.056(3)	−0.002(2)	−0.003(2)	0.002(2)
O(3)	0.051(3)	0.027(3)	0.051(4)	0.001(3)	0.000(3)	0.003(2)
O(4)	0.041(2)	0.034(2)	0.046(3)	0.003(2)	0.000(2)	0.000(2)
O(5)	0.037(2)	0.041(2)	0.044(3)	−0.001(2)	0.000(2)	−0.007(2)
O(6)	0.048(3)	0.021(3)	0.042(3)	0.005(2)	−0.008(2)	−0.004(3)
O(7)	0.055(3)	0.035(3)	0.035(3)	−0.003(2)	−0.003(2)	0.001(3)
O(8)	0.045(3)	0.035(3)	0.055(3)	−0.001(2)	0.001(2)	−0.001(2)
OT(1)	0.036(3)	0.036(3)	0.060(3)	0.001(2)	0.000(2)	0.001(2)
OT(2)	0.036(3)	0.042(3)	0.054(3)	−0.001(2)	0.001(2)	0.001(2)

Table 5. Cell Parameters, Refined Atomic Coordinates, and Isotropic Temperature Factors from $RbTi_{0.927}Nb_{0.056}Er_{0.017}OPO_4$ by Neutron Data at RT

Cell Parameters			
a (Å) = 12.9708(2)	b (Å) = 6.5064(1)	c (Å) = 10.5733(2)	V (Å^3) = 892.32(3)

atom	x	y	z	B_{iso}
Ti(1)	0.373(1)	0.491(5)	0.437(3)	0.5(2)
Nb(1)	0.373(1)	0.491(5)	0.437(3)	0.5(2)
Er(1)	0.373(1)	0.491(5)	0.437(3)	0.5(2)
Ti(2)	0.247(2)	0.268(3)	0.692(2)	0.5(2)
Er(2)	0.247(2)	0.268(3)	0.692(2)	0.5(2)
P(1)	0.499(1)	0.335(1)	0.695(2)	0.61(8)
P(2)	0.1812(5)	0.495(3)	0.946(2)	0.61(8)
Rb(1)	0.3864(8)	0.786(1)	0.765(1)	1.87(9)
Rb(2)	0.1058(9)	0.690(1)	0.519(1)	1.87(9)
O(1)	0.4837(8)	0.484(2)	0.588(1)	0.60(2)
O(2)	0.512(1)	0.456(1)	0.821(1)	0.60(2)
O(3)	0.398(1)	0.201(2)	0.717(1)	0.60(2)
O(4)	0.594(1)	0.197(2)	0.677(1)	0.60(2)
O(5)	0.110(1)	0.311(2)	0.981(1)	0.60(2)
O(6)	0.116(1)	0.690(2)	0.921(1)	0.80(2)
O(7)	0.251(1)	0.542(2)	0.064(1)	0.60(2)
O(8)	0.254(1)	0.458(2)	0.834(1)	0.60(2)
OT(1)	0.223(1)	0.960(2)	0.079(1)	0.60(2)
OT(2)	0.222(1)	0.045(2)	0.827(1)	0.60(2)

Reliability Factors
$\chi^2 = 1.65\%$, $R_p = 5.39\%$, $R_{wp} = 6.82\%$, R_f factor = 4.74%, Bragg R-factor = 6.20%

The volume of the unit cell was larger because of the increase in the atomic radii of Er^{3+}, but the distribution of this larger volume was not the same for all three cell parameters: a and b were 0.19 and 0.14% longer, respectively, and c was 0.05% shorter than the param-

eters of the $Rb_{0.855}Ti_{0.955}Nb_{0.045}OPO_4$ crystal. Our main aim was to obtain reliable information about the distribution of the small concentration of Er and Nb cations in the structure (we take advantage of the very different Fermi lengths for neutrons of Ti (3.37 fm) and Nb (7.054
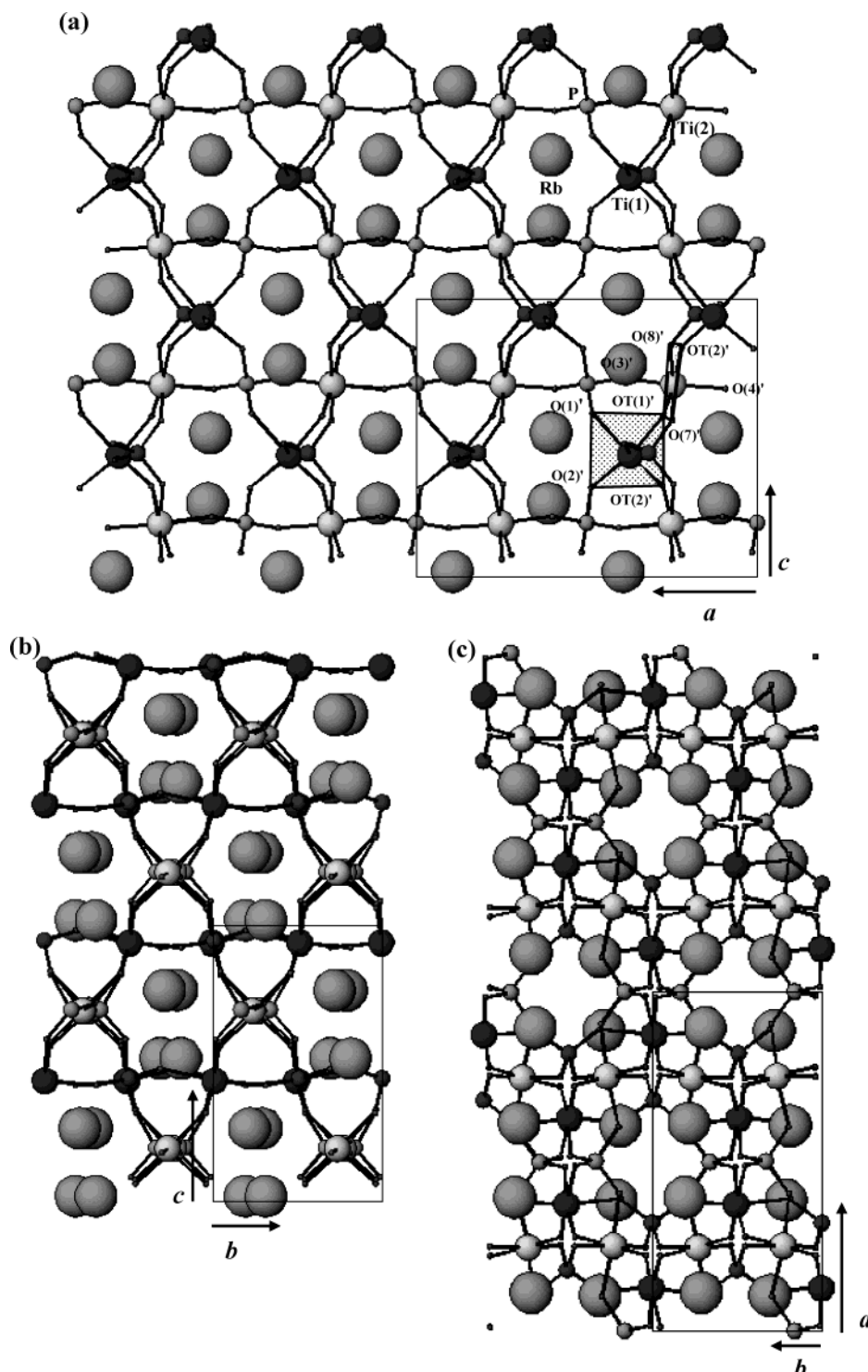
Figure 2. View of the structure of the RTP family of crystals illustrating the connected paths formed by alternating $Ti(1)O_6$ and $Ti(2)O_6$ octahedra. Projections parallel to (a) [010], (b) [100], and (c) [001] directions.

fm) or Er (8.03 fm). With this objective in mind, and using a random distribution of Nb and Er among Ti sites as a starting point, we performed different sets of Rietveld refinements of the NPD data for different models of the distribution of dopants. As expected, Nb and Er only went to Ti sites in the $RbTi_{0.927}Nb_{0.056}Er_{0.017}OPO_4$ structure. We also checked for the possibility of vacant oxygen or rubidium. All the atomic positions, including oxygen or rubidium sites, were fully occupied. This was in contrast to some vacant rubidium sites found in the RTP:Nb crystal. In our $RbTi_{0.927}Nb_{0.056}Er_{0.017}OPO_4$ crystal, within a resolution of ~1%, we found that the two Rb sites were fully occupied.

When we impose that Er and Nb cations randomly substituted the two Ti sites, the reliability factors were $R_{wp} = 6.88\%$, $R_f = 4.79\%$, and $R_{bragg} = 6.29\%$. However, when we allowed for an inhomogeneous distribution of the dopants, the reliability factors clearly improved. When we fitted the occupation factors, the refinements always converged to the same scenario: Nb atoms are only substituted Ti(1) atoms at the center of the Ti(1)-O_6 octahedra. On the other hand, Nb cations did not

Table 6. Selected Bond Distances in
$Rb_{0.855}Ti_{0.955}Nb_{0.045}OPO_4$ (X-rays) and
$RbTi_{0.927}Nb_{0.056}Er_{0.017}OPO_4$ (Neutrons)[a]

	$Rb_{0.855}Ti_{0.955}Nb_{0.045}OPO_4$	$RbTi_{0.927}Nb_{0.056}Er_{0.017}OPO_4$
Ti(1)−O(1)	2.123(6)	2.15(3)
Ti(1)−O(2)[i]	1.963(6)	1.96(3)
Ti(1)−O(5)[ii]	2.083(6)	2.15(4)
Ti(1)−O(6)[iii]	2.013(6)	1.97(4)
Ti(1)−OT(1)[iii]	1.926(6)	1.95(3)
Ti(1)−OT(2)[ii]	1.751(6)	1.74(3)
⟨Ti(1)−O⟩	1.977	1.99
P(1)−O(1)	1.516(6)	1.50(2)
P(1)−O(2)	1.567(6)	1.56(2)
P(1)−O(3)	1.539(6)	1.58(2)
P(1)−O(4)	1.566(5)	1.53(2)
⟨P(1)−O⟩	1.547	1.54
Rb(1)−O(1)	3.042(6)	2.99(2)
Rb(1)−O(2)	2.725(7)	2.75(1)
Rb(1)−O(3)[v]	2.795(6)	2.75(1)
Rb(1)−O(5)[ii]	3.006(6)	3.00(2)
Rb(1)−O(6)[vi]	3.396(6)	3.41(2)
Rb(1)−O(7)[ii]	3.227(6)	3.23(2)
Rb(1)−O(8)	2.844(6)	2.83(2)
Rb(1)−OT(1)[iii]	3.181(6)	3.22(2)
Rb(1)−OT(2)[v]	2.792(6)	2.79(2)
⟨Rb(1)−O⟩	3.000	2.99
Ti(1)−Rb(1)[iii]	4.085(2)	
Ti(1)−Rb(2)[vi]	3.699(2)	

	$Rb_{0.855}Ti_{0.955}Nb_{0.045}OPO_4$	$RbTi_{0.927}Nb_{0.056}Er_{0.017}OPO_4$
Ti(2)−O(3)	2.023(6)	2.03(3)
Ti(2)−O(4)[iv]	2.024(5)	2.01(2)
Ti(2)−O(7)[iii]	1.953(6)	2.00(2)
Ti(2)−O(8)	2.005(6)	1.95(3)
Ti(2)−OT(1)[iii]	1.777(6)	1.77(2)
Ti(2)−OT(2)	2.049(6)	2.06(2)
⟨Ti(2)−O⟩	1.972	1.97
P(2)−O(5)	1.547(5)	1.56(2)
P(2)−O(6)	1.548(6)	1.55(2)
P(2)−O(7)	1.552(6)	1.56(2)
P(2)−O(8)	1.514(6)	1.54(2)
⟨P(2)−O⟩	1.540	1.55
Rb(2)−O(1)[vii]	2.755(6)	2.74(2)
Rb(2)−O(2)[ii]	3.107(7)	3.12(2)
Rb(2)−O(3)[ii]	3.166(7)	3.19(2)
Rb(2)−O(4)[iv]	2.989(5)	3.02(2)
Rb(2)−O(5)[viii]	2.832(5)	2.82(2)
Rb(2)−O(7)[ii]	3.029(6)	3.00(2)
Rb(2)−O(8)[ii]	3.170(6)	3.19(2)
Rb(2)−OT(1)[iii]	2.792(6)	2.75(2)
Rb(2)−OT(2)[ii]	3.104(6)	3.16(2)
⟨Rb(2)−O⟩	2.993	2.99
Ti(2)−Rb(1)[ix]	3.676(2)	
Ti(2)−Rb(2)[x]	3.936(3)	

[a] i: $-x + 1, -y + 1, z - \frac{1}{2}$. ii: $-x + \frac{1}{2}, y + \frac{1}{2}, z - \frac{1}{2}$. iii: $-x + \frac{1}{2}, z - \frac{1}{2}$. iv: $x - \frac{1}{2}, -y + \frac{1}{2}, z$. v: $x, y + 1, z$. vi: $x + \frac{1}{2}, -y + \frac{3}{2}, z$. vii: $x - \frac{1}{2}, -y + \frac{3}{2}, z$. viii: $-x, -y + 1, z - \frac{1}{2}$. ix: $x, y - 1, z$. x: $\frac{1}{2} - x, y - \frac{1}{2}, z + \frac{1}{2}$.

substitute Ti atoms of the $Ti(2)O_6$ octahedra. We were able to refine the occupation factors of Nb and Er freely, with the only constraints that the Ti octahedra were fully occupied and had no vacant sites and that the concentrations of these cations in the structure were those given by EPMA analyses. The occupation factors therefore converged to the values given in Table 3: in our $RbTiOPO_4$ sample (doped with 5.6% Nb and 1.7% Er), Nb cations exclusively substituted Ti(1) sites. For Er, the refinements converged to the occupations 0.014-(6) for Er(1) and 0.020(6) for Er(2). According to the errors, this is undistinguishable from or equivalent to Er being equally distributed between Ti(1) and Ti(2) (a fraction of 0.017 in each octahedra). However, the limit of the sensitivity of the technique is the highest for the small concentration of Er, and the corresponding relative errors are very important.

Second-Harmonic Generation. SHG relative efficiency is defined as the ratio between η_{sample} and η_{KTP}, where η is the ratio between the powers measured at 532 and 1064 nm. In the studies of $Rb_{0.855}Ti_{0.955}Nb_{0.045}$-$OPO_4$ and $RbTi_{0.927}Nb_{0.056}Er_{0.017}OPO_4$, this was 1.2 and 0.7, respectively. These results are referred to KTP, now that the parameters of KTP are well-established in the literature.[26]

The SHG relative efficiency of $Rb_{0.855}Ti_{0.955}Nb_{0.045}$-$OPO_4$ was around 20% higher than that of KTP. As we showed in a previous study,[17] the SHG relative efficiency of RTP doped with Nb increases as the concentration of Nb increases until it reaches a maximum for a Nb concentration of around 4−5 at. % in the crystal. For higher concentrations of Nb, the SHG relative efficiency decreases. Our results therefore entirely agree with those of our previous studies of SHG relative efficiency in RTP:Nb crystals. Finally, the SHG relative efficiency of the sample containing Nb and Er was lower (0.7). If we compare this result with the expected one from a sample of RTP doped only with Nb and containing a similar concentration of this ion,[17] we can see that the SHG relative efficiency is clearly lower. This may be due to the presence of Er in the sample because this ion has a significant absorption of light from $^4I_{15/2}$ to $^2H_{15/2}$ manifolds in the green region.[17−19] We found, however, that this absorption did not dramatically decrease SHG relative efficiency, so we can conclude that the NLO properties of this crystal are as good as those of the RTP crystal.

Discussion

Figure 2 shows the structure of this family of compounds. It is a network of chains of very distorted TiO_6 octahedra linked by PO_4 octahedra with periodic bond chains of $-PO_4-TiO_6-$ in the a direction and along the $a-c$ diagonal (Figure 2a). Ti(1) and Ti(2) octahedra alternate along the c direction to form helicoidal chains of linked TiO_6 octahedra (Figure 2a,b). Each $Ti(1)O_6$ octahedron shares two corners with $Ti(2)O_6$ octahedra through the OT(1) and OT(2) oxygens and the other four corners with PO_4 tetrahedra. If we take the plane containing the central Ti atom and the two OT oxygens as the equatorial plane of the Ti octahedra, then the equatorial plane of $Ti(1)O_6$ is almost parallel to the (010) plane, the c axis is almost parallel to the OT(1)[iii]−OT-(2)[ii] (see Table 6) vector, and the a axis is approximately parallel to the OT(1)[iii]−O(1) vector. The O(5)[ii] and O(6)[iii] atoms are out of the plane and bonded to Ti(1) along a line almost parallel to the b axis. In the Ti(2) octahedron, the equatorial plane is almost parallel to the (100) plane and formed by O(7), O(8), OT(1), and OT(2) atoms. The c axis is approximately parallel to the O(8)−OT-(1)[iii] vector and the apical O(3) and O(4)[iv] atoms are bonded to Ti(2) along a line almost parallel to the a axis. The typical long and short Ti−O bonds in the structure of KTP isomorphs are maintained, but if we compare their distances with those of pure RTP crystals, the Ti-(1)−OT(1) and Ti(2)−OT(2) distances are shorter in these new crystals, while the Ti(1)−OT(2) and Ti(2)−OT(1) distances are longer (see Table 6 and ref 3). The PO_4 tetrahedra are not very different from those of the

Table 7. Distortion TiO_6 Parameters and SHG Efficiency for KTP Family Compounds

	$\Delta_{Ti(1)-O}$	$\Delta_{Ti(2)-O}$	$d(Ti(1)-OT(1))$	$d(Ti(1)-OT(2))$	$d(Ti(2)-OT(1))$	$d(Ti(2)-OT(2))$	η_{sample}/η_{KTP}	ref
$KTiOAsO_4$	37	26	1.957(16)	1.735(16)	1.770(19)	2.097(19)	>1	3
$Rb_{0.855}Ti_{0.955}Nb_{0.045}OPO_4$	37	22	1.926(6)	1.751(6)	1.777(6)	2.049(6)	1.2	
$KTiOPO_4$	44	33	1.981(3)	1.716(3)	1.733(3)	2.092(3)	1	3
$RbTiOPO_4$	47	22	1.973(4)	1.714(4)	1.737(4)	2.094(4)	0.7	3, 14
$RbTi_{0.927}Nb_{0.056}Er_{0.017}OPO_4$	43	23	1.95(3)	1.74(3)	1.77(2)	2.06(2)	0.7	
$KSnOPO_4$	11	7	1.957(5)	1.961(5)	1.978(6)	1.975(7)	≈0	28

358 undoped RTP compounds. The RbO_9 cages occupy the
359 channels left by the network of the TiO_6 octahedra and
360 PO_4 tetrahedra along the *c* direction (see Figure 2c).
361   It is of interest to note that in this family of crystals
362 the $Ti(1)O_6$ octahedra are larger than the $Ti(2)O_6$
363 octahedra. Another feature of the selective distribution
364 of Nb is that only the former is occupied: the ionic
365 radius of Nb^{5+} is slightly larger than the radius of Ti^{4+}
366 (0.64 and 0.605 Å, respectively[28]). Taking into account
367 the much larger radius of Er^{3+} ions (0.881 Å[28]), the
368 average Ti−O bond lengths in Table 6 for $RbTi_{0.927}$-
369 $Nb_{0.056}Er_{0.017}OPO_4$ appear to suggest that Er has a
370 preference for Ti(1) sites over Ti(2) sites. However,
371 because of the importance of the errors associated to
372 the Ti−O bond lengths in this powder sample, we cannot
373 draw any conclusions from the differences observed.
374   Now we turn to the Rb vacants sites in the RTP:Nb
375 crystal. Although EPMA measurements did not estab-
376 lish the stabilization of vacancies of Rb in both types of
377 crystals, the refinement of the structures gives a clear
378 loss of Rb in the crystals that contained only Nb. This
379 is an interesting aspect of doping RTP with Nb: the
380 ability of the material to self-compensate electrically for
381 the pentavalent substitution through the loss of Rb
382 atoms. The mean Rb−O bond length was greater in the
383 $Rb_{0.855}Ti_{0.955}Nb_{0.045}OPO_4$ structure than in the pure
384 RTP.[4] This is consistent with the expansion of the cages
385 in the structure caused by the loss of Rb atoms. In
386 particular, the average Rb(1)−O distance (3.000 Å) in
387 the $Rb_{0.855}Ti_{0.955}Nb_{0.045}OPO_4$ crystal (which has Rb
388 vacant sites) was slightly higher than that in the
389 $RbTi_{0.927}Nb_{0.056}Er_{0.017}OPO_4$ and RTP crystals (2.99 and
390 2.994 Å, respectively). This was not observed in the Rb-
391 $(2)O_9$ cage, which had the same average Rb(2)−O bond
392 length in all three materials: 2.993 Å (with Rb vacant
393 sites), 2.99 Å (Nb, Er), and 2.992 Å (RTP). This indicates
394 that when doping with pentavalent Nb^{5+} ions, Rb vacant
395 sites are created mainly at the Rb(1) site. This inter-
396 pretation also agrees with the different occupations of
397 the Rb(1) and Rb(2) sites refined in $Rb_{0.855}Ti_{0.955}Nb_{0.045}$-
398 OPO_4 (see Table 3).
399   Although Nb enters preferentially at the Ti(1) site in
400 both crystal structures, the Ti(1) and Ti(2) sites are very
401 similar crystallographically. If we define the distortion
402 parameter $\Delta_d = (1/6)\sum_{n=1-6}\{[d(Ti-O)_n - \langle d(Ti-O)\rangle]/$
403 $\langle d(Ti-O)\rangle\}^2$, we can compare the distortion of the TiO_6
404 octahedra for our two crystals with that of other
405 compounds of the KTP family (see Table 7). In all cases,
406 doped and undoped, Ti(1) octahedra were more distorted
407 than Ti(2) octahedra. Moreover, in the present concen-
408 tration range, the distortion in the $Ti(2)O_6$ octahedra
409 of RTP was not modified by doping with Nb or co-doping
410 with Nb and Er. In our opinion the preference for Nb^{5+}
411 ions to occupy Ti(1) sites has an electrostatic origin

412 rather than a steric one. If we compare the Ti−Rb bond
413 distances in the $Rb_{0.855}Ti_{0.955}Nb_{0.045}OPO_4$ and $RbTi_{0.927}$-
414 $Nb_{0.056}Er_{0.017}OPO_4$ structures, we can see that these
415 distances are quite shorter for the Ti(2) cation than for
416 the Ti(1) cation (see Table 6). This implies that the
417 electronic repulsion in the Ti(2) position is higher than
418 that in the Ti(1) position. Consequently, Nb^{5+} tends to
419 occupy Ti(1) positions to avoid this electrostatic repul-
420 sion, an interpretation that is reinforced by the very
421 similar radius of the Ti^{4+} and Nb^{5+} ions, while in the
422 case of Er^{3+}, because of its lower electrical charge, this
423 effect has not been observed.
424   It is believed that the markedly short Ti(1)−OT(2) and
425 Ti(2)−OT(1) bonds are partially responsible for the
426 optical nonlinearity in this family of compounds.[29]
427 Phillips et al.[30] showed that the lengthening of the Ti-
428 (1)−OT(2) bond to the same distance as the Ti(1)−OT-
429 (1) bond was associated with a dramatic loss in SHG.
430 Another example is $KSnOPO_4$ (KSnP), where Ti is
431 substituted by Sn. In this case the SnO_6 octahedra are
432 practically undistorted and, interestingly, the SHG
433 efficiency drops by a factor of 70%. Although KSnP is
434 isostructural with KTP, its structure is much closer to
435 that of the centrosymmetric phase *Pnan*.[31] In our case,
436 by looking at the Ti−OT bonds in $Rb_{0.855}Ti_{0.955}Nb_{0.045}$-
437 OPO_4 and $RbTi_{0.927}Nb_{0.056}Er_{0.017}OPO_4$, we did not find
438 a clear or direct relationship between the difference in
439 these bonds and SHG efficiency (see Table 7). We are
440 therefore led to conclude that other factors also have a
441 great influence on nonlinearity (such as modifications
442 in the electronic structure due to doping). Notice, finally,
443 that chemical bond calculations made by Xue and
444 Zhang[32−34] for the KTP structure suggest that the K(2)-
445 O_9 and $P(2)O_4$ groups are also responsible for the
446 nonlinear optical properties of this compound.

Conclusions

448   We have solved the structures of $Rb_{0.855}Ti_{0.955}Nb_{0.045}$-
449 OPO_4 and $RbTi_{0.927}Nb_{0.056}Er_{0.017}OPO_4$, two new isos-
450 tructurals of $KTiOPO_4$, and measured their SHG re-
451 sponse. The main characteristic of these structures is
452 that we obtained the enantiomorphic image of pure
453 RTP. In both structures, the Nb and Er cations only
454 went to Ti sites, and the refinements of the structures
455 confirmed that in both materials Nb cations exclusively
456 substituted Ti(1) sites. On the other hand, the situation
457 for Er was undistinguishable, as it was equally distrib-

(28) Shannon, R. D. *Acta Crystallogr.* **1976**, *A32*, 751.

(29) Zumsteg, F. C.; Bierlein, J. D.; Gier, T. E. *J. Appl. Phys.* **1976**, *47*, 4980.
(30) Phillips, M. L.; Gier, T. E.; Eddy, M. M.; Keder, N. L.; Stucky, G. D.; Bierlein, J. D. *Solid State Ionics* **1989**, *32−33*, 147.
(31) Thomas, P. A.; Glazer, A. M.; Watts, B. E. *Acta Crystallogr.* **1990**, *B46*, 333.
(32)] Xue, D.; Zhang, S. *Appl. Phys. Lett.* **1997**, *70*, 943.
(33) Xue, D.; Zhang, S. *Physica B* **1999**, *262*, 78.
(34) Xue, D.; Zhang, S. *J. Solid State Chem.* **1999**, *142*, 156.

uted between Ti(1) and Ti(2) sites. We believe that this preference for Nb ions to occupy Ti(1) sites has an electrostatic origin rather than a steric one. Another remarkable feature was the ability of the material to self-compensate electrically for the pentavalent substitution through the loss of Rb atoms in the crystal that contained only Nb, but when Er^{3+} was also present, this charge self-compensation was not necessary.

Measurements of SHG relative efficiency show that both these crystals are excellent nonlinear optical materials. In $RbTi_{0.927}Nb_{0.056}Er_{0.017}OPO_4$, we observed the absorption of green light by Er, but this did not decrease SHG efficiency dramatically. Comparison of the nonlinear optical properties of these crystals with those of other members of the structural family shows that there is no clear or direct relationship between the difference in Ti−OT bonds, or the distortion of the TiO_6 octahedra, and SHG efficiency. Other factors also have a strong influence on nonlinearity.

CM034044T

Initial Page

Papers